AD NUMBER

AD212064

LIMITATION CHANGES

TO:

Approved for public release; distribution is unlimited.

FROM:

**Distribution authorized to U.S. Gov't. agencies and their contractors;
Administrative/Operational Use; JAN 1959. Other requests shall be referred to Army Ballistic Research Lab., Aberdeen Proving, Ground, MD.**

AUTHORITY

BRL D/A ltr dtd 22 Apr 1981

BRL

REPORT NO. 1062
JANUARY 1959

THE MAGNUS FORCE ON A SHORT BODY AT SUPERSONIC SPEEDS

A. S. PLATOU

DEPARTMENT OF THE ARMY PROJECT NO. 5B03-03-008
ORDNANCE RESEARCH AND DEVELOPMENT PROJECT NO. TB3-1036

BALLISTIC RESEARCH LABORATORIES
ABERDEEN PROVING GROUND, MARYLAND

DISCLAIMER NOTICE

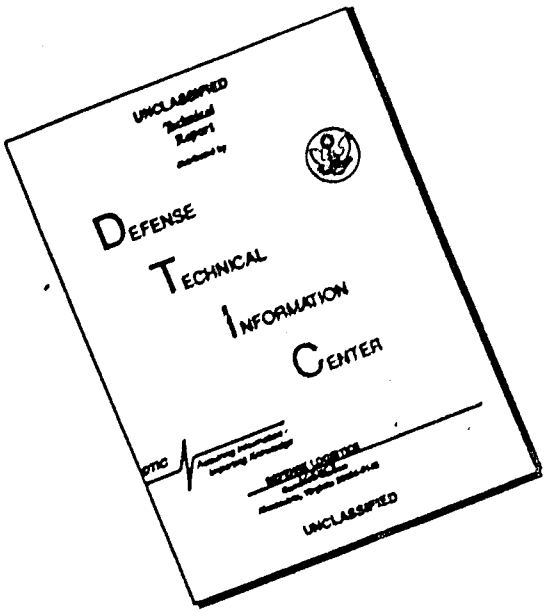

THIS DOCUMENT IS BEST QUALITY AVAILABLE. THE COPY FURNISHED TO DTIC CONTAINED A SIGNIFICANT NUMBER OF PAGES WHICH DO NOT REPRODUCE LEGIBLY.

B A L L I S T I C R E S E A R C H L A B O R A T O R I E S

REPORT NO. 1062

JANUARY 1959

THE MAGNUS FORCE ON A SHORT BODY AT SUPERSONIC SPEEDS

A. S. Platou

Requests for additional copies of this report will be made direct to ASTIA

Department of the Army Project No. 5B03-03009
Ordnance Research and Development Project No. TB3-1838

A B E R D E E N P R O V I N G G R O U N D, M A R Y L A N D

B A L L I S T I C R E S E A R C H L A B O R A T O R I E S

REPORT NO. 1062

ASPlatou/sec
Aberdeen Proving Ground, Md.
January 1959

THE MAGNUS FORCE ON A SHORT-BODY AT SUPERSONIC SPEEDS

ABSTRACT

The recent information obtained through the testing of spinning models in the Aberdeen supersonic wind tunnels has led to a better understanding of the behavior of the Magnus force generated on rotating projectiles. Data have been obtained at Mach 2.0 on a low fineness ratio (3.2) body of revolution. Spin rates up to 40,000 r.p.m. ($\frac{\omega d}{U} \approx .40$) have been used which cover the spin range used by conventional bullets and shell.

The Magnus force is dependent on the boundary layer conditions and with most of the configurations tested the Magnus force is linear with spin and angle of attack in the low angle of attack range. It is only when the configuration base corner is rounded that the Magnus force becomes non-linear with spin and angle of attack.

TABLE OF CONTENTS

TABLE OF SYMBOLS

a = speed of sound

d = model diameter

ℓ = model length

Ma = Mach number = $\frac{U}{a}$

P_o = stagnation pressure

q = dynamic pressure = $\frac{1}{2} \rho U^2$

Re = Reynolds number = $\frac{\rho U d}{\mu}$

R_ℓ = Reynolds number = $\frac{\rho U \ell}{\mu}$

T_o = stagnation temperature

U = test section air velocity

α = angle of attack

ψ = angle of yaw

ρ = test section air density

μ = test section air viscosity

ω = spin rate of model (plus is clockwise looking upstream)

ν = $\frac{\omega d}{U}$

k_N = normal force coefficient = $\frac{N}{\rho U^2 d^2}$

k_m = pitching moment coefficient = $\frac{m}{\rho U^2 d^3}$

k_F = Magnus force coefficient = $\frac{F}{\rho U^2 d^2 \nu}$ (plus is to left looking upstream)

k_T = Magnus moment coefficient = $\frac{T}{\rho U^2 d^3 \nu}$ (plus is plus force ahead of moment center)

K_F = Ballistics Magnus force coefficient = $\frac{F}{\rho U^2 d^2 \nu \sin \alpha}$

K_F = $\frac{dk_F}{d\alpha}$ when k_F is linear in α and α is small and in radians.

C.P. = Magnus force center of pressure location from base in calibers

INTRODUCTION

At the time of publication of BRL Report 994[1], describing the Magnus data obtained on a model of a 30mm aircraft bullet, many questions concerning the Magnus force were left unanswered.* Several of these questions have been answered during the elapsed interval and these findings are presented in this report. The questions are as follows:

1. A turbulent boundary layer existed on the model during the previous tests. How different is the Magnus force produced on a spinning body having a laminar boundary layer from that produced with a turbulent boundary layer?

2. A Magnus theory based on the movement of the laminar boundary layer due to spin has been advanced by Martin[2]. Does this theory agree with experiments?

3. In order to obtain satisfactory Magnus data with a turbulent boundary layer, it is necessary that transistion be fixed with respect to the model surface. This usually requires a transition strip. Does forcing transition change the Magnus force from that obtained with natural transition?

4. The Magnus force on the 30mm aircraft bullet is non-linear both with spin and angle of attack. What is the reason for this?

Questions 1 and 2 require a laminar boundary layer over the complete model surface. This limits the angle of attack to fairly low values where complete laminar boundary layers can exist. Also the transition problem mentioned in Question 3 is important only at low angles of attack where transition is not completely controlled by the body angle of attack. The non-linearity mentioned in Question 4 can be considered in two parts. a) The low angle of attack region where sign reversal (negative Magnus force) of the Magnus force is possible and b) the high angle of attack

*The unclassified results of BRL Report 994 are given in Appendix I.

region where the data are only non-linear with angle of attack. It is believed the two types of non-linearity are created by separate causes.

From the above it can be seen that most of the questions deal with the low angle of attack region and can be conveniently separated from the high angle of attack region. This report deals only with the low angle of attack problems.

INSTRUMENTATION

The models and instrumentation used for obtaining the data are similar to that described in reference 1.* The models are 2-inch diameter steel bodies mounted on precision ball bearings. An air turbine mounted in the base of the model is used for spinning the model, and the aerodynamic forces are recorded using a four component (double pitch and double yaw) strain gage balance read only while the model is decelerating (i.e. the air supply to the turbine is turned off).

One important change was made in the instrumentation since the data reported in reference 1 were obtained. The power to the strain gages was changed from 60 cycle, 6 volt A.C. to 6 volt D.C. with filter condensers in each signal lead to damp out signal oscillations due to tunnel turbulence. Also automatic drum recorders were used to record the yawing moment signals versus spin rate while the pitching moment signals were manually recorded from multi-scale Brown instruments as before. The above changes increased the accuracy of the data and decreased the tunnel time required for running the tests.

A further refinement at the start of the testing was made in order to simplify the data reduction procedure. Whenever the balance was installed in the tunnel the model angle of yaw and angle of attack positions were shifted slightly until zero angle of yaw and zero angle of attack were indicated by the strain gage readings (an adjustable yaw strut was used for changing the angle of yaw). Next the balance was rolled slightly until the yaw hinge lines were in the angle of attack plane so that the normal force interaction with the yawing moments was nil. Exactly zero interaction on both gages is impossible due to a 1° angle between the two yaw hinge lines as indicated by the calibrations.

---

*The description of the instrumentation is reprinted as Appendix II of this report for the convenience of those readers not having ready access to classified reports.

A typical set of reduced data obtained from this instrumentation is shown in Figure 2. Each curve represents the Magnus force and center of pressure for a constant angle of attack from 40,000 rpm down to zero rpm. It will be noticed that the data are slightly asymmetric with angle of attack, and at the present time it is believed that this asymmetry is due to small changes in the lateral normal force caused by small changes in the model yaw during any one spin period. These changes in yaw could be due to play in the model bearings. The amount of play necessary to create the asymmetry shown ($\frac{M.F.}{\rho U^2 d^2} = .0005$) can be computed from the obtained data. The change in angle of yaw ($\Delta\Psi$) is $\frac{.0005}{k_N}$ where k_N for this model, Ma = 2.0, is .021 (Figure 3). $\Delta\Psi$ is then $.024^o$. The bearings are 3" apart so the play in each bearing need only be $\pm$ .0006".

One further indication that the asymmetry is caused by a change in the lateral normal force is that the asymmetry is much greater in the rear yawing moment data than in the front yawing moment. Since the rear strain gage is further from the normal force c.p., any change in the normal force would have the largest effect on the rear yawing moment.

To partly overcome the remaining asymetric deficiency, the data at plus and minus angles of attack have been averaged. This makes the present Magnus force coefficient ($\frac{F}{\rho U^2 d^2}$) accurate to approximately $\pm$ .0003, while the center of pressure is accurate to approximately 1 caliber.

TEST RESULTS

The model of the 30mm aircraft bullet has a very complicated aerodynamic shape which makes it difficult to analyze any data obtained on the configuration. This is especially true if the data are non-linear as with the obtained Magnus data. As a result it was decided to begin testing with a simple aerodynamic shape (called the basic body, Figure 1).

For the turbulent boundary layer case, transition was forced to occur at a fixed distance from the nose by using an emery strip cemented to the surface of the body (Figure 1). Fixing the transition line was necessary for, as discussed in reference 1, the zero spin yawing moments are dependent on the model roll position if transition occurs at various axial positions around the surface of the model.

However, forced transition at other than zero angle of attack creates slightly different conditions than those occurring with natural transition (Figure 4). Also the forced turbulent boundary layer characteristics are likely to be different from the natural boundary layer characteristics. The tripping mechanism is certainly different and the velocity profiles, shear forces and effective Reynolds number may be different. Since the Magnus force is generated by viscous action in the boundary layer the above thoughts on differences between forced and natural transition should be studied carefully.

During the testing of the basic body, (Figure 1), three sizes of grit were used as transition strips to obtain boundary layers having different characteristics (Figures 7 to 10). Also the body was tested without a trip ring to obtain laminar boundary layer data (Figure 5 and 6). The Magnus force data obtained under these conditions at $\omega d/U = .4$ are compared in Figure 11. The magnitude of the Magnus force decreases with grit size and the Magnus force generated in the laminar boundary layer case is less than that generated in any of the turbulent boundary layer cases. Figure 11 also shows that in all boundary layer cases on the basic

body the Magnus force is linear with angle of attack. The data at lower spin rates show that the Magnus force is also linear with spin and the values of k_f shown in Figure 11 will hold for any spin rate at or below $\omega d/U = .4$. This shows conclusively that the negative and non-linear Magnus force obtained on the 30mm bullet is not caused by changes in the boundary layer characteristics.

Martin's theory [2] develops an expression for the Magnus force by determining the asymmetry created in the boundary layer displacement thickness due to the spin, and then applying the slender body theory to the resulting asymmetric body. Martin's theory is elementary in that many assumptions must be made and it may only be applicable in the simplest cases. Simple body configuration, low angle of attack, and a laminar boundary layer are essential. The theory disregards the nose and substitutes a blunt, open-ended cylinder, the length of which is different from that of the nose plus body. In calculating the Magnus force on an ogive cylinder configuration, Martin uses a theoretical cylinder length equal to one half the nose length plus the actual cylinder length. The expressions developed for Magnus force and its center of pressure are:

$$K_F = \frac{10.33\left(\frac{l}{d}\right)^2}{(R_l)^{1/2}}$$

$$\frac{C.P.}{l} = .40$$

For the configuration shown in Figure 1, the theoretical cylinder length based on Martin's method is 2.45. Using this l/d, $K_F = .050$ and C.P. = .98 cal. for the test Reynolds number. This agrees better than expected with the laminary experimental coefficients of $K_F = .054$ and C.P. = 1 ± 1 obtained at Ma = 2.0, $R_l = 1.58 \times 10^6$. At other Mach numbers the agreement is not as good; however, it is within the range of error one might expect, (Table I). Kelley and Thacker[3] and [4]

of Inyokern, have extended the theory to include a radial pressure gradient effect and a skin friction term. They also consider the next higher order terms in spin which makes the Magnus force non-linear in spin. Their results are as follows:

$$K_F = \frac{\pi \left(\frac{l}{d}\right)^2}{2 \left(R_l\right)^{1/2}} \left[7.834 - 16.526 \left(\frac{\omega d}{2U}\right)^2 \left(\frac{l}{d}\right)^2 + \ldots.\right]$$

$$\frac{C.P.}{l} = .40 + .375 \left(\frac{\omega d}{2U}\right)^2 \left(\frac{l}{d}\right)^2 + \ldots.$$

A plot of the above equations with $l/d = 2.45$ cal. is shown in Figure 12. The experimental data on the basic configuration with laminar boundary layer show constant K_F with spin and do not agree with Kelly's results. The experimental center of pressure data are too inaccurate to indicate a trend with spin rate.

Most shell or bullets which are fired from guns require modifications to the streamlined shape of Figure 1 in order that they may be successfully launched against enemy targets. These modifications, in most cases, create discontinuities in the configuration surface thereby complicating the existing flow field.

The 30mm aircraft bullet, which has several of these discontinuities (Figure 13), was tested here previously and the Magnus force results (Figure 14 and 15) were quite different from the linear results obtained on the basic body. This configuration generates Magnus forces which are extremely non-linear in spin and angle of attack. Under some angle of attack and spin conditions the direction of the Magnus force is negative rather than positive. The Magnus force on the basic body (Figure 1) showed linear results, therefore the cause of the reversal must be one or more of the discontinuities.

A process of elimination of the various non-streamlined components of the shape showed that the rounded base corner is creating the negative Magnus forces and the non-linearities at low angle of attack. (Figure 16,

17, and 18). This result was very surprising and unexpected for the rounded base appears to be one of the less significant changes in the configuration. The blunt nose, the rotating band, and the crimping groove are physically much larger changes in the streamline shape; however, these changes have a lesser, although significant, influence on the Magnus force. These three changes have their largest influence when used with the rounded base. In this case the Magnus force becomes more negative than with just the rounded base. It has also been determined that the rounded base produces the negative Magnus force with both a laminar and a turbulent boundary layer. The laminar case is shown in Figure 19.

A numerical computation of the pressure difference on the rounded portion of the base which would produce the observed difference in Magnus force has been made. The pressure difference is approximately .004 times the stagnation pressure while the static pressure ratio at the base is approximately .128. This means that only a small change in pressure is required to account for the change in Magnus force and it is entirely feasible that this pressure difference could be produced by the rounded base.

During the review of this report it was pointed out to the author that a series of tests (5) made in the Aberdeen Aerodynamics Range showed a large difference in the Magnus moment due to the addition of a hemispherical base to the square based body (Figure 20). Assuming that the change in moment is due to a force acting on the hemisphere the force must act in the negative direction in order to produce the observed change in moment. From this reasoning these tests support the evidence that rounded bases create negative Magnus forces.

Shadowgraph pictures, (Figure 21) taken during the Aerodynamics Range tests on the hemispherical base show that the flow over the base is similar to that over the aft portion of a sphere. The flow overexpands as it attempts to follow the hemispherical surface and then must recompress in order to adjust to the wake flow. During this process the flow separates from the hemispherical surface, with the exact location

of the separation being controlled by several factors. The model spin may be one of these factors and it is conceivable that the influence of the spin may adjust the separation point and also the pressures acting on the hemispherical surface such that negative forces are created.

Although the Magnus Force center of pressure data are not sufficiently accurate to pinpoint the force under various conditions, it is possible to state that under all conditions tested the center of pressure is aft of the forward yaw gage (2-1/4 cal. forward of the base) and in most cases it is located on the aft third of the body. This means that the Magnus force distribution is concentrated on the aft portion of the body so that changes in the nose configurations should not influence the force except through possible changes in the boundary layer characteristics. No conclusions on the motion of the center of pressure with angle of attack and spin can be made due to the inaccuracy of the data.

No significant variation in pitching moment or normal force due to spin of the configuration was noticed during any of the tests.

CONCLUSIONS

A study of the Magnus force on low fineness ratio bodies leads to the following conclusions:

1. The Magnus force generated on the basic body with a laminar boundary layer is less than the Magnus force generated on the same body with a turbulent boundary layer.

2. The Magnus force generated on the basic body with a forced turbulent boundary layer is dependent on the size of emery grit used for the transition strip.

3. Martin's theory agrees with the laminar boundary layer data obtained within the expected accuracy of the theory.

4. The Magnus force center of pressure is located on the aft portion of the body.

5. A rounded base can create a negative and non-linear Magnus force.

6. Modifications to a streamlined body such as blunt nose, a rotating band or a crimping groove influences the Magnus force to a significant but lesser degree than does a rounded base.

7. A square based body has a positive Magnus force and the force is linear with spin and with angle of attack up to at least 5°.

8. The normal force is not influenced by spin.

A. S. Platou

A. S. PLATOU

REFERENCES

1. Platou, A. S., and Sternberg, J. "The Magnus Characteristics of a 30 mm Aircraft Bullet". BRL Rpt. 994. (Confidential) Sept. 1956.

2. Martin, John C. "On Magnus Effects Caused by the Boundary Layer Displacement Thickness on Bodies of Revolution at Small Angles of Attack". BRL Rpt. 870, Revised. June 1955.

3. Kelly, Howard R. "An Analytical Method for Predicting the Magnus Forces and Moments on Spinning Projectiles". NAVORD Tech Memo 1634. August 1954.

4. Kelly, Howard R., and Thacker, G. Robert "The Effect of High Spin on the Magnus Force on a Cylinder at Small Angles of Attack". NAVORD Rpt. 5036, February 1956.

5. Deitrick, Ralph E. "Effect of a Hemispherical Base on the Aerodynamic Characteristics of Shell". BRL Memo Rpt. 947. November 1955.

TABLE I

Ma	K_F Exper.	C.P. Exper. Cal. from base	R_ℓ*	K_F* Theory	C.P.* Theory Cal. from base
1.57	.055	.75 ± 1	1.85×10^6	.046	.98
2.00	.054	1 ± 1	1.58×10^6	.050	.98
2.47	.063	1-1/4 ± 1	1.58×10^6	.050	.98
3.02	.066	1 ± 1	1.58×10^6	.050	.98

*Based on $\ell/d = 2.45$

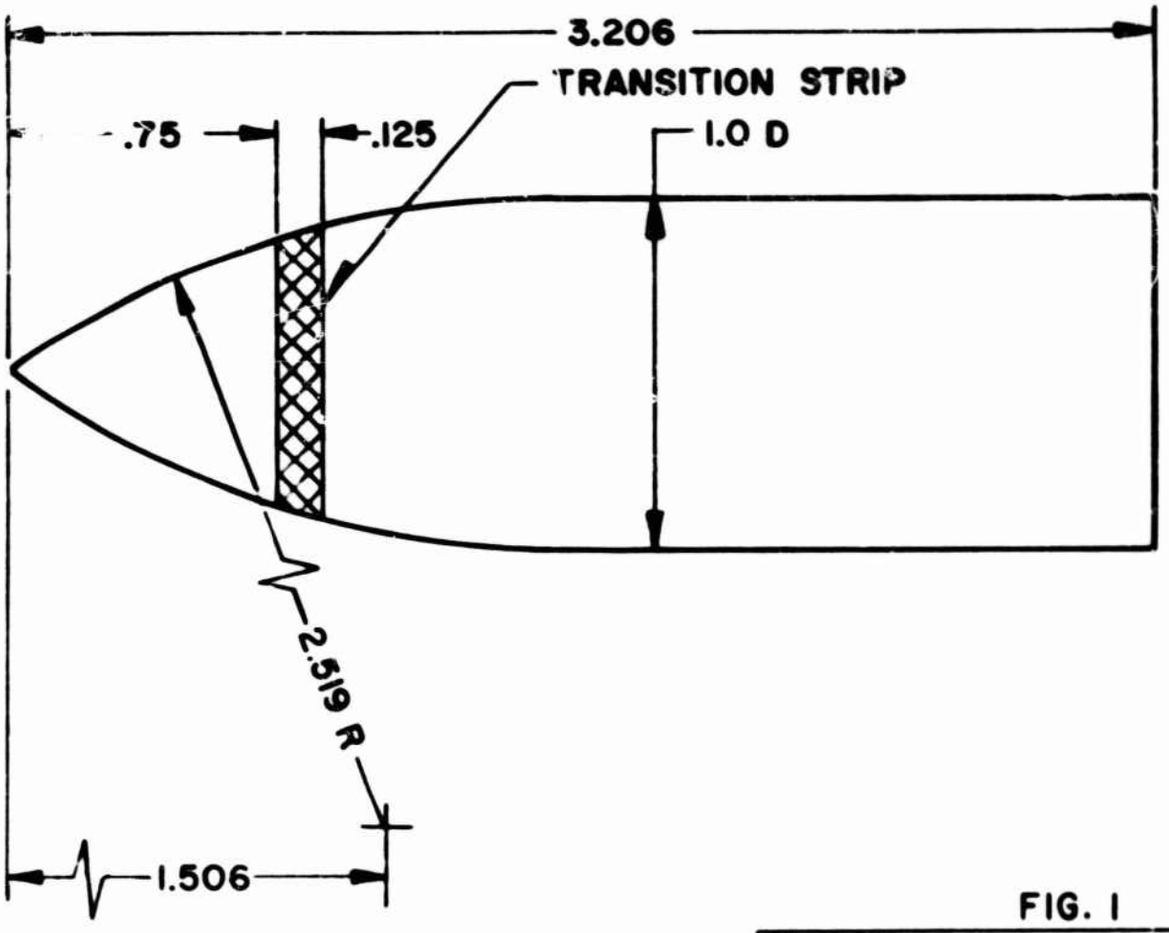

FIG. 1

BASIC BODY

SUPERSONIC WIND TUNNELS, LAB.
BALLISTIC RESEARCH LAB., A.P.G., MD.

NOTE:
ALL DIMENSIONS IN CALIBERS
1 CALIBER = 2.00 INCHES

A TYPICAL SET OF MAGNUS DATA OBTAINED ON THE BASIC BODY

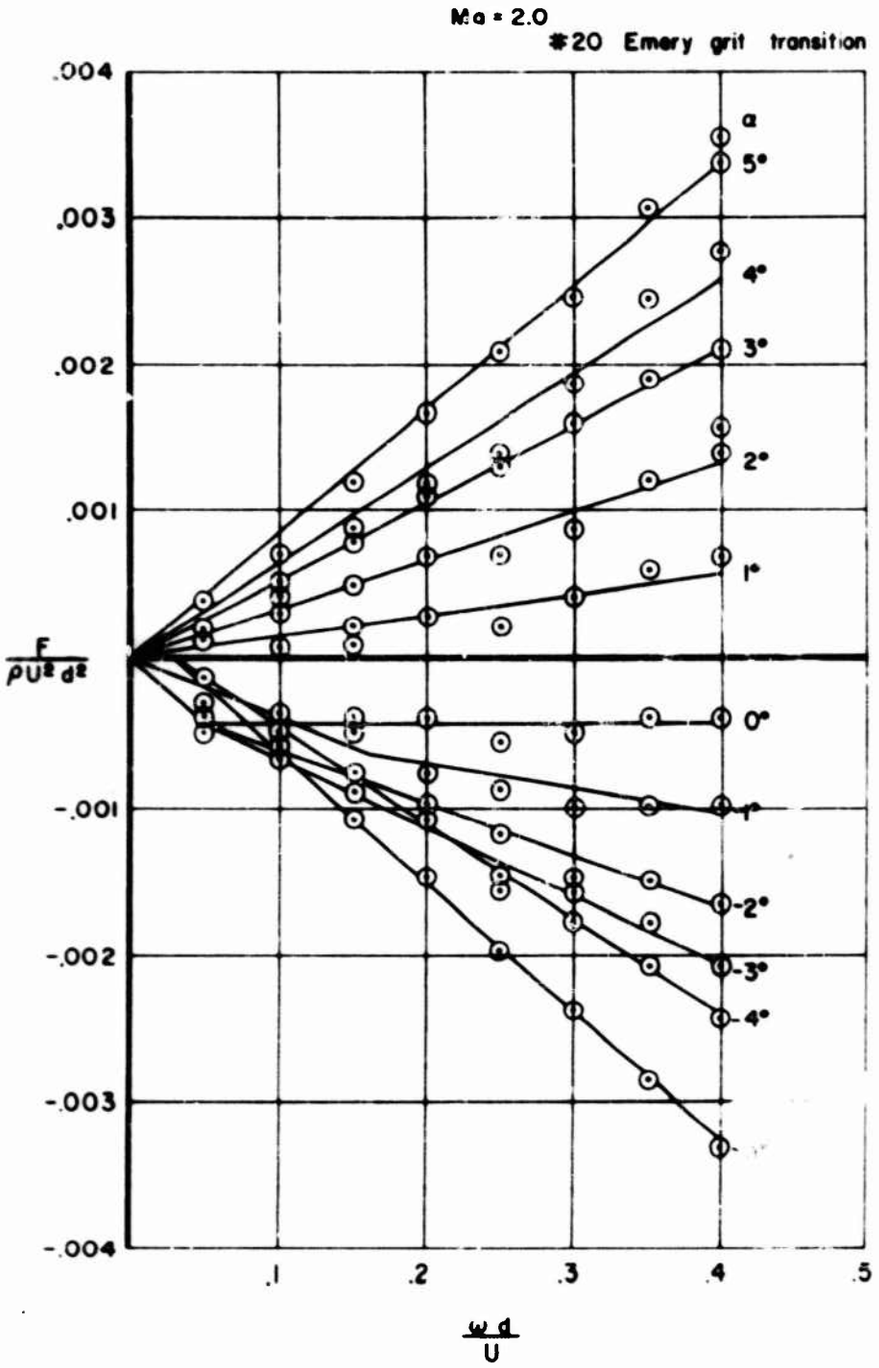

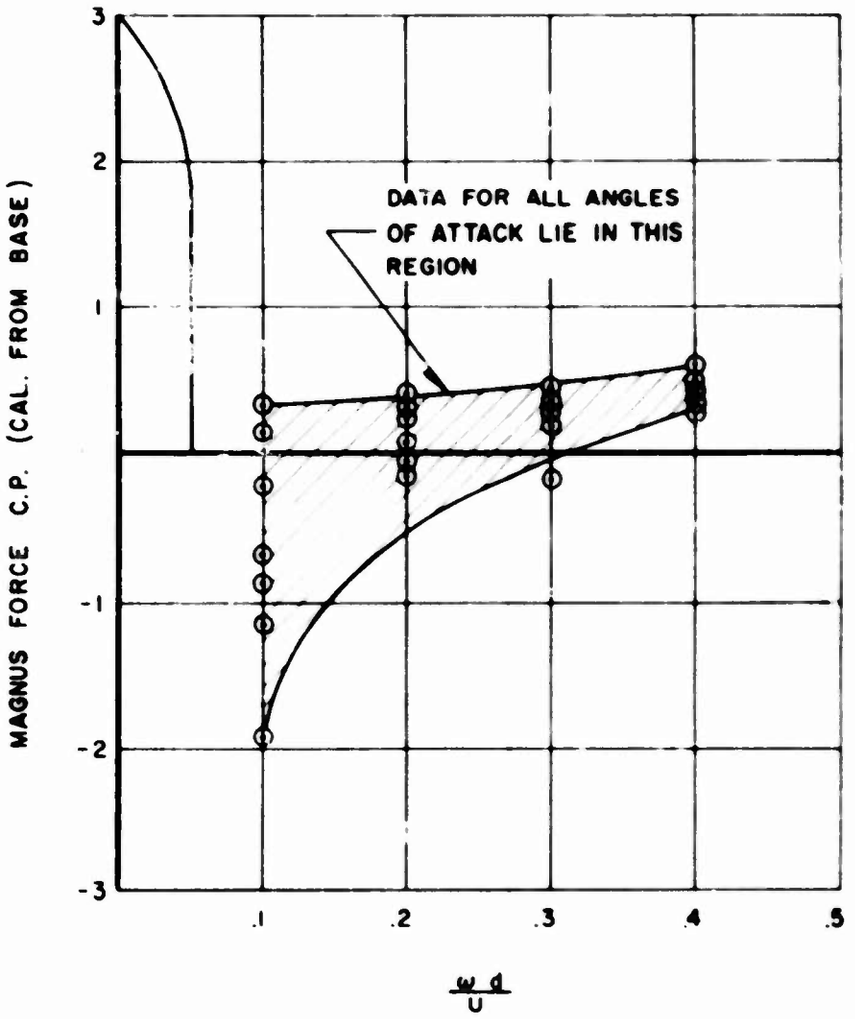

FIG. 2

THE NORMAL FORCE AND PITCHING MOMENT ON THE BASIC BODY

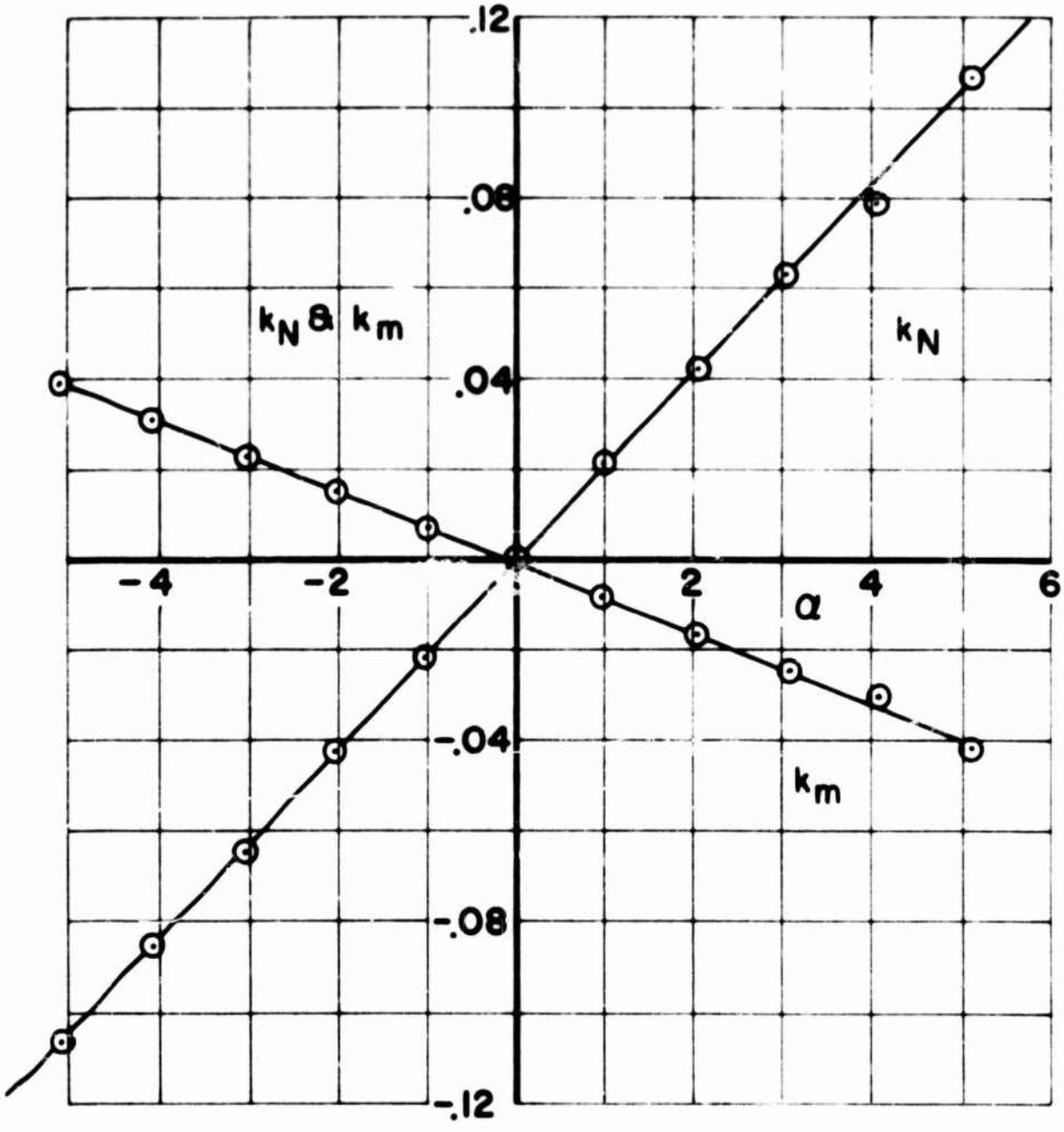

MOMENT IS ABOUT FRONT PITCH
GAGE: 2.3 CAL. AHEAD OF BASE

FIG. 3

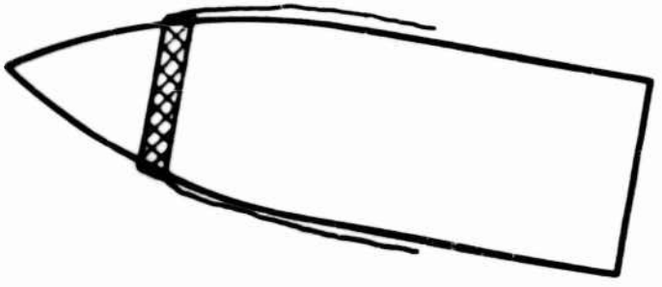

FORCED TRANSITION

NATURAL TRANSITION

FIG. 4

FORCED AND NATURAL TRANSITION

SUPERSONIC WIND TUNNELS, LAB.
BALLISTIC RESEARCH LAB., A.P.G., MD.

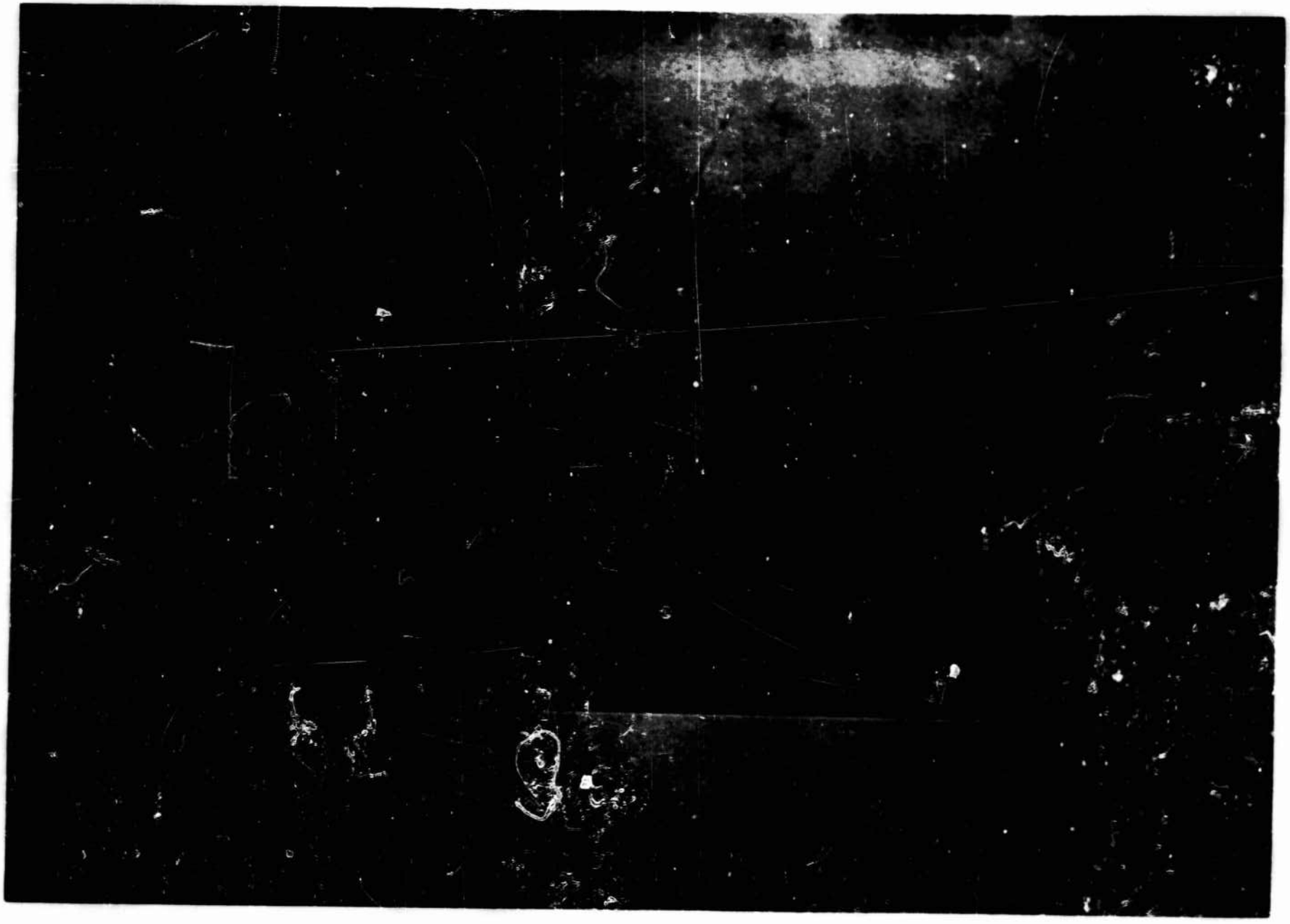

Fig. 5 Basic Configuration with Laminar Boundary Layer

$Ma = 2.0 \quad Re = .65 \times 10^6 \quad \frac{\omega d}{U} = 0 \quad \alpha = 0^\circ$

Fig. 6 Basic Configuration with Laminar Boundary Layer

$M_a = 2.0 \quad Re = .65 \times 10^6 \quad \frac{\omega d}{U} = 0 \quad \alpha = 5^\circ$

Fig. 7 Basic Configuration with No. 20 Emery Transition Strip

$Ma = 2.0 \quad Re = .65 \times 10^6 \quad \frac{\omega d}{U} = 0 \quad \alpha = 0$

Fig. 8 Basic Configuration with No. 20 Emery Transition Strip

$M_\infty = 2.0 \quad Re = .65 \times 10^6 \quad \frac{\omega d}{U} = 0 \quad \alpha = 5^\circ$

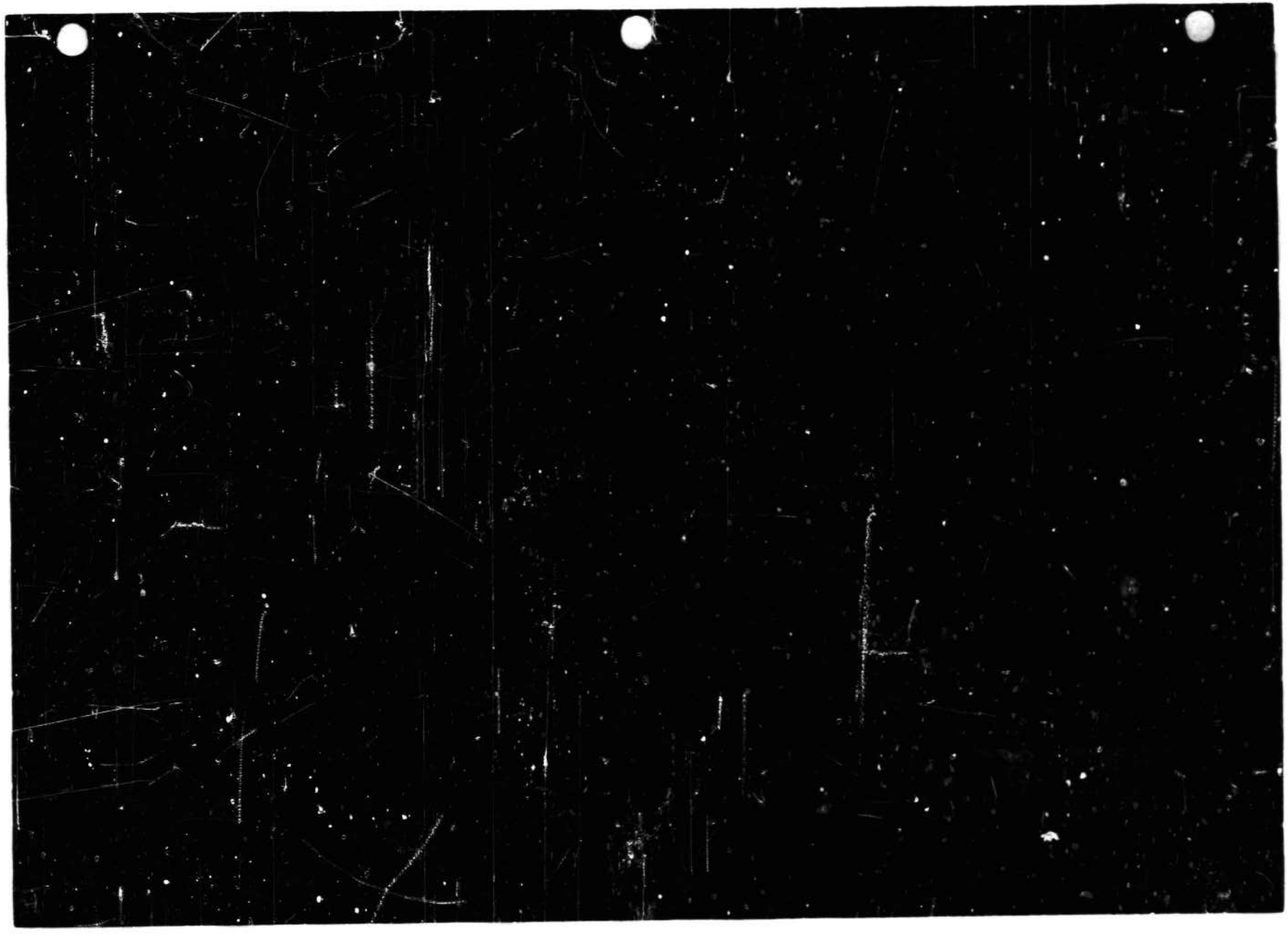

Fig. 9 Basic Configuration with No. 40 Transition Strip

$Ma = 2.0 \quad Re = .65 \times 10^6 \quad \frac{\omega d}{U} = 0 \quad \alpha = 0^\circ$

Fig. 10 Basic Configuration with No. 80 Emery Transition Strip

$Ma = 2.0 \quad Re = .65 \times 10^6 \quad \frac{\omega d}{U} = 0 \quad \alpha = 0^o$

EFFECT OF BOUNDARY LAYER ON THE MAGNUS FORCE OF THE BASIC BODY

Ma = 2.0 Re = .65 X 10^6

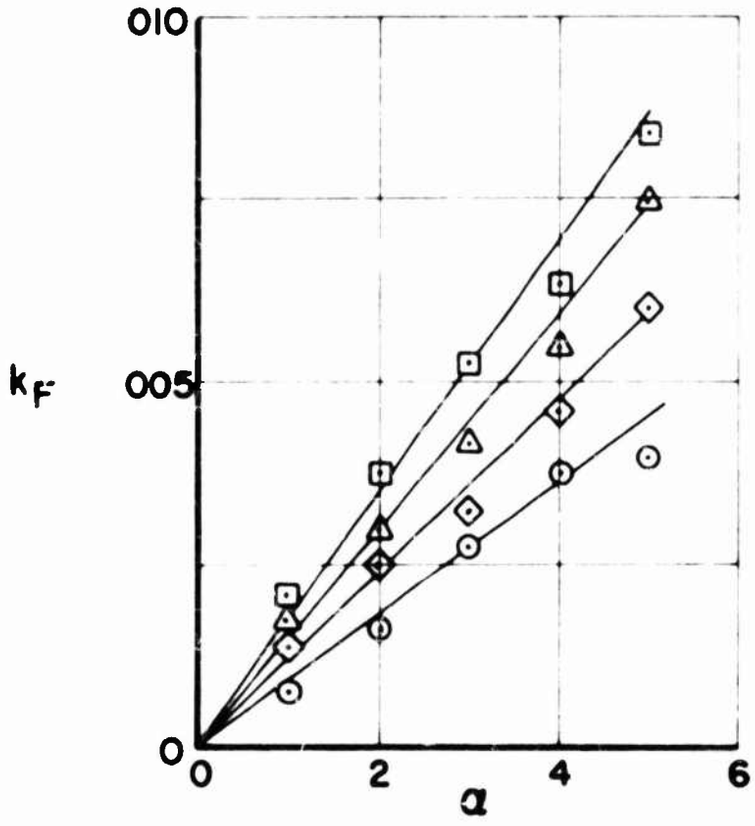

○ LAMINAR BOUNDARY LAYER

□ #20 TRANSITION STRIP (LARGEST GRIT)

△ #40 TRANSITION STRIP (MEDIUM GRIT)

◇ #80 TRANSITION STRIP (SMALLEST GRIT)

FIG. 11

THE MAGNUS FORCE PREDICTED BY KELLY AND THACKER

$\frac{l}{d} = 2.45$ $\quad R_\theta = 1.58 \times 10^6$

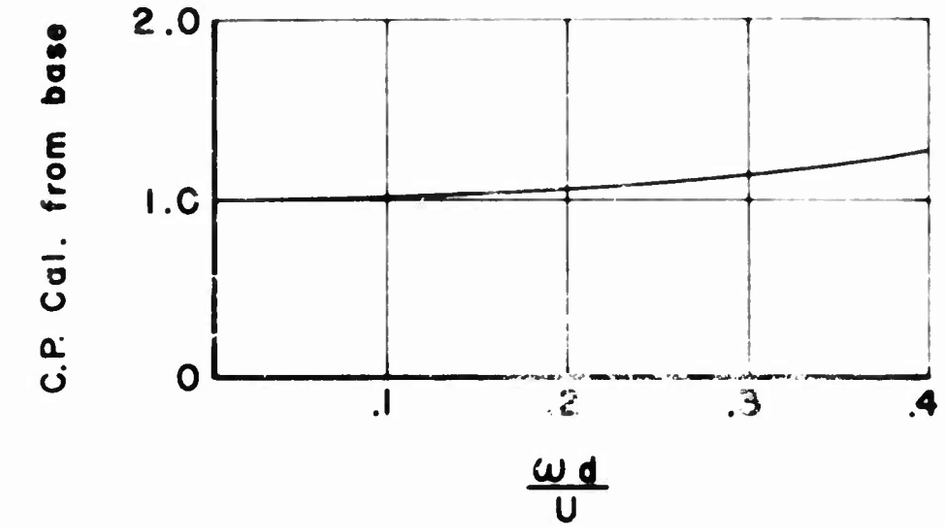

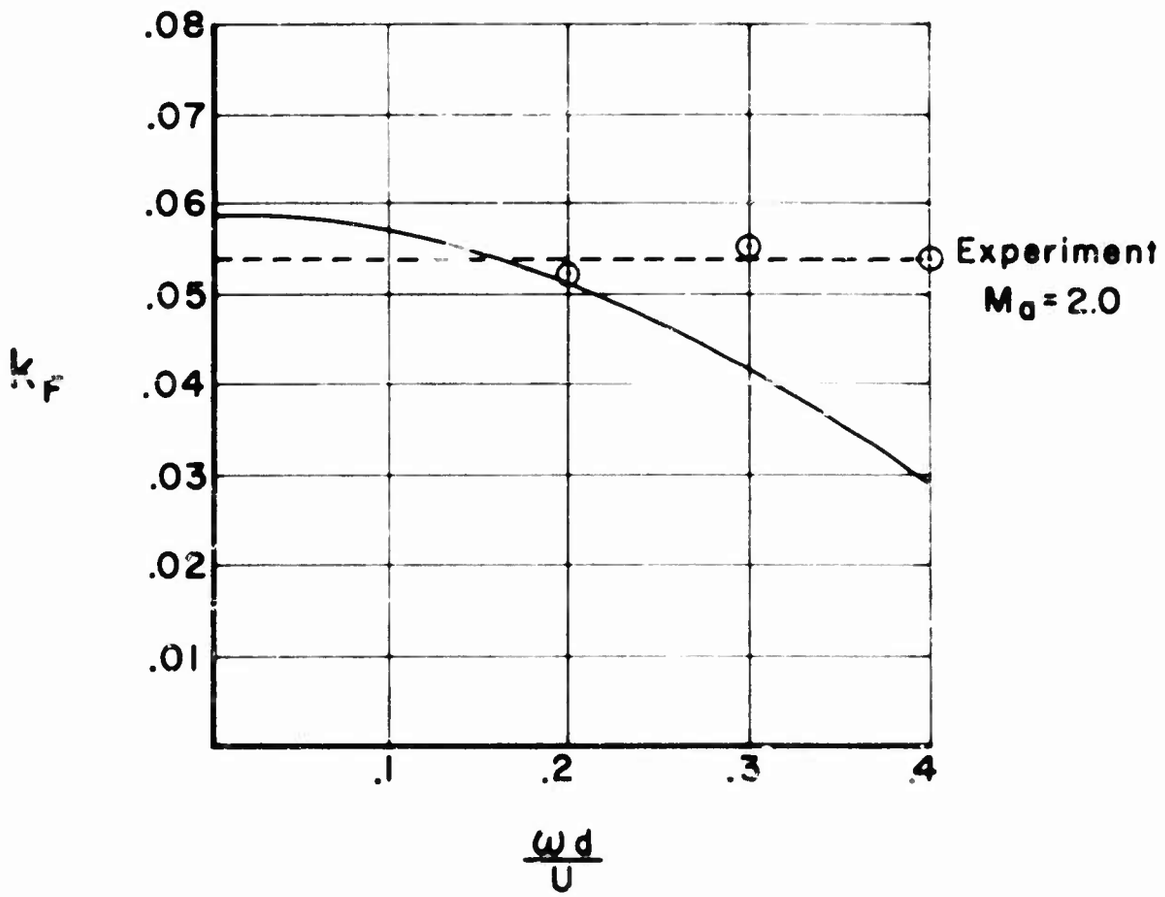

FIG. 12

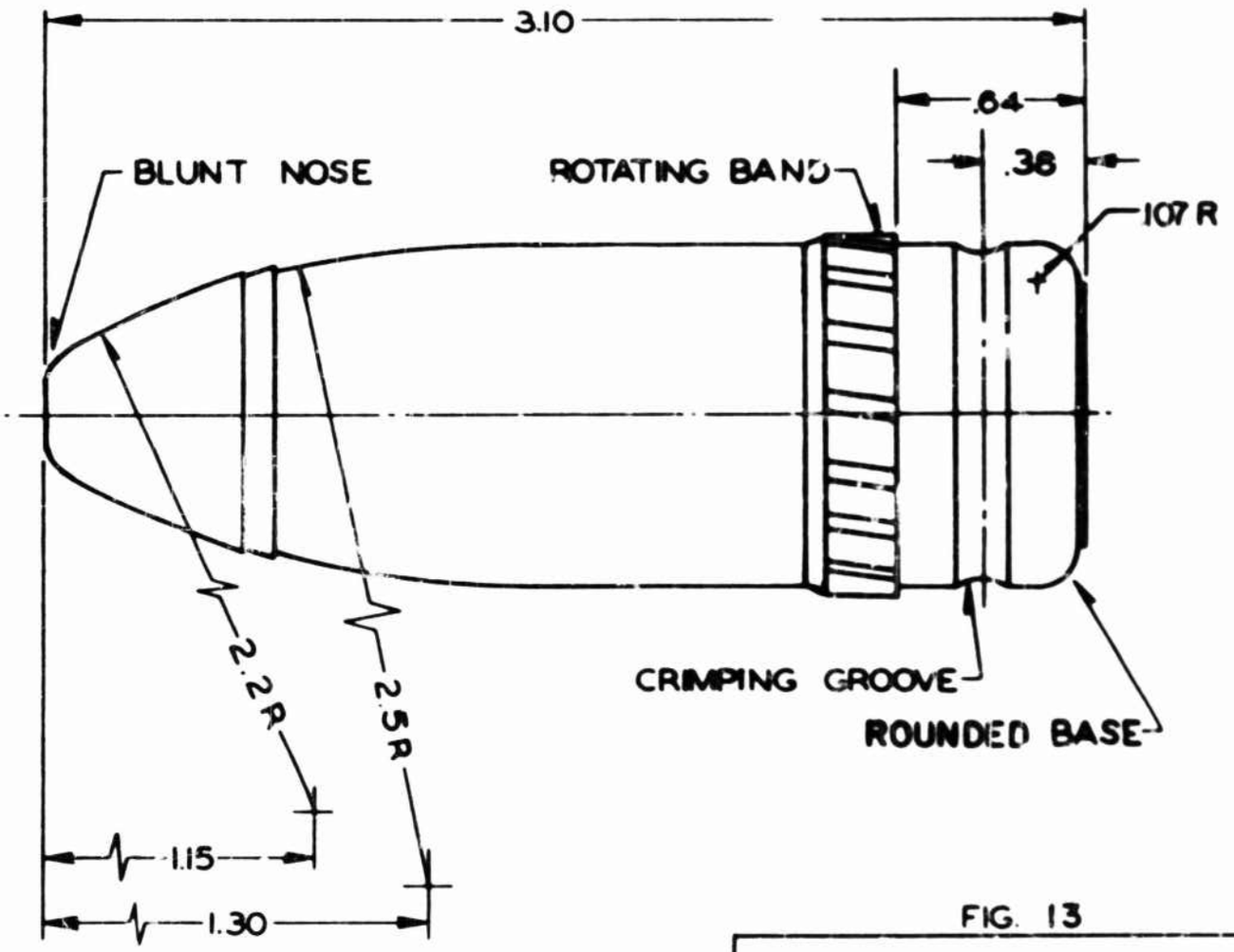

FIG. 13

30MM AIRCRAFT BULLET

SUPERSONIC WIND TUNNELS, LAB.
BALLISTIC RESEARCH LAB., A.P.G., MD.

NOTE:
ALL DIMENSIONS IN CALIBERS
1 CALIBER 2.00 INCHES

THE MAGNUS FORCE ON THE 30 MM AIRCRAFT BULLET

$M_\infty = 2.0$ $R_e = .65 \times 10^6$ $\frac{\omega d}{U} = .2$

FORCED TRANSITION AT $\frac{x}{d} = .75$ #40 EMERY

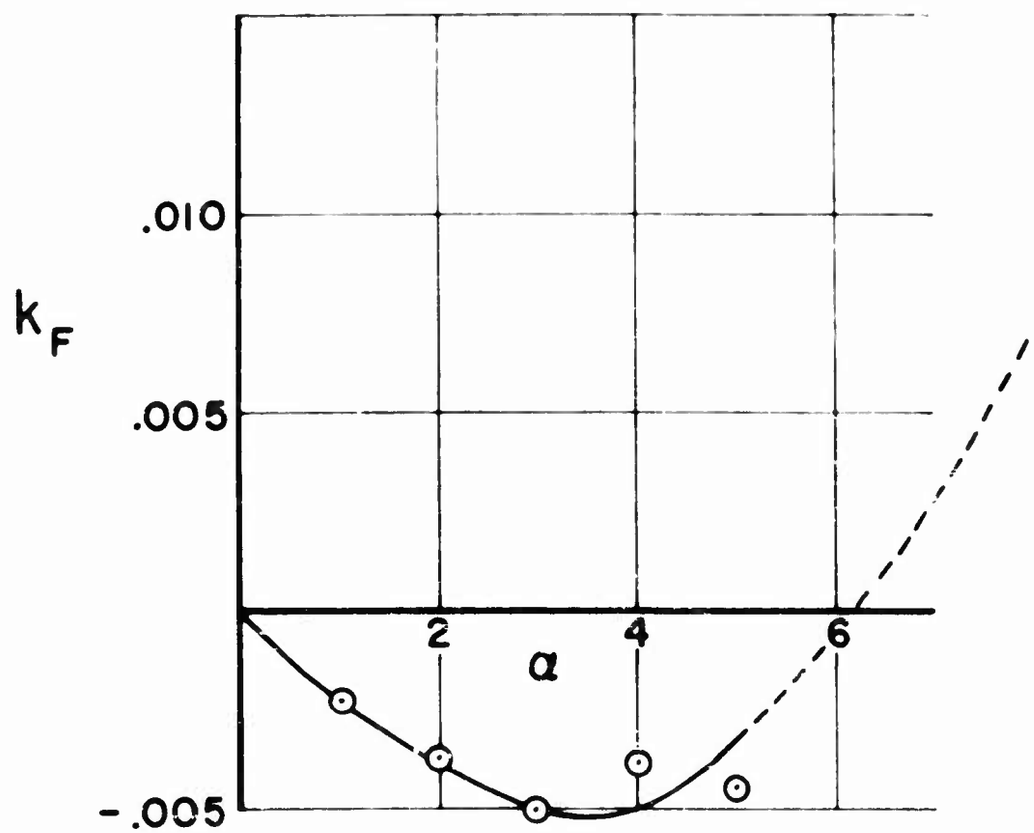

FIG. 14

THE MAGNUS FORCE ON THE 30 MM AIRCRAFT BULLET

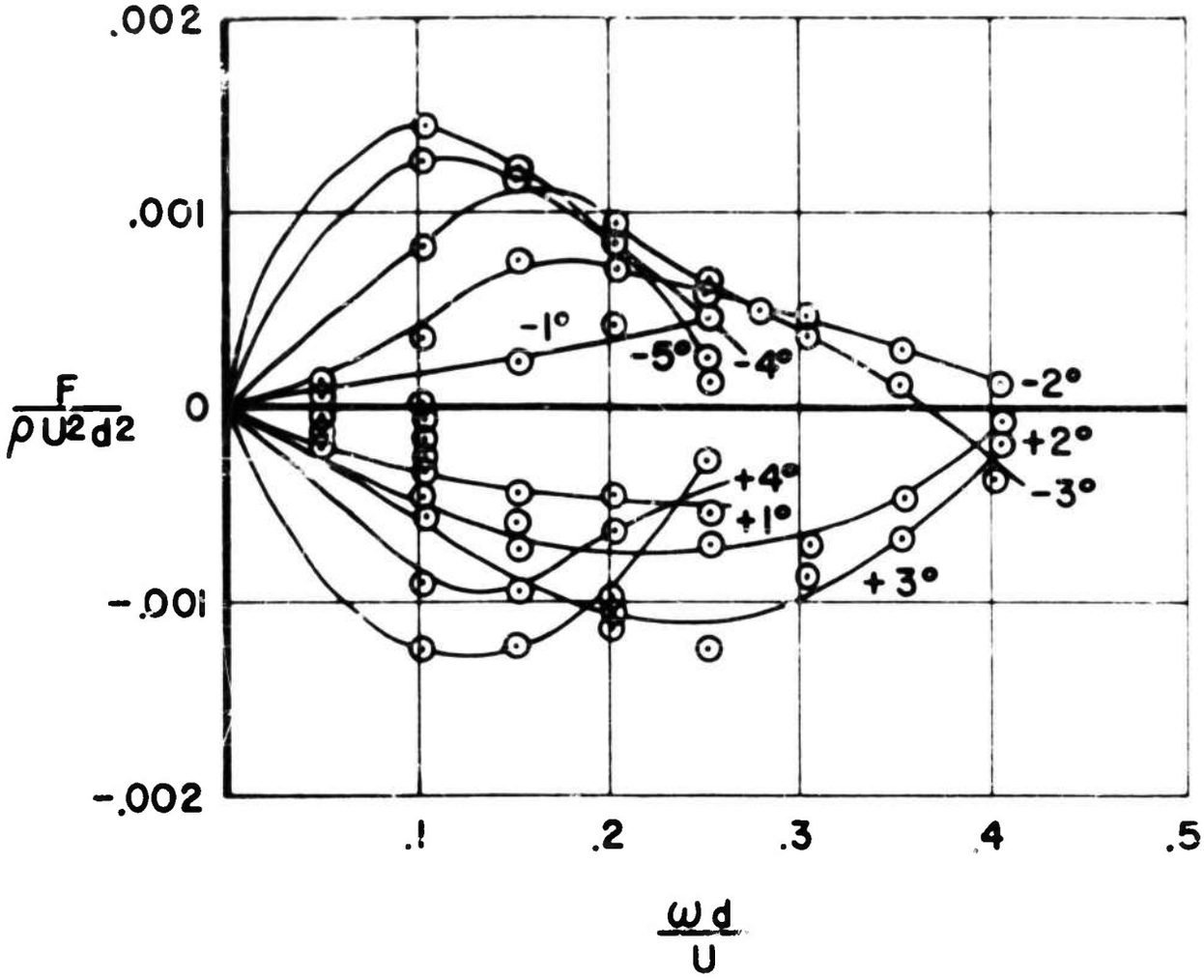

FIG. 15

THE EFFECT OF A ROUNDED BASE ON MAGNUS FORCE

$M_\infty = 2.0$ $R_e = .65 \times 10^6$ $\frac{\omega d}{U} = .20$

FORCED TRANSITION AT $\frac{x}{d} = .75$ #40 EMERY

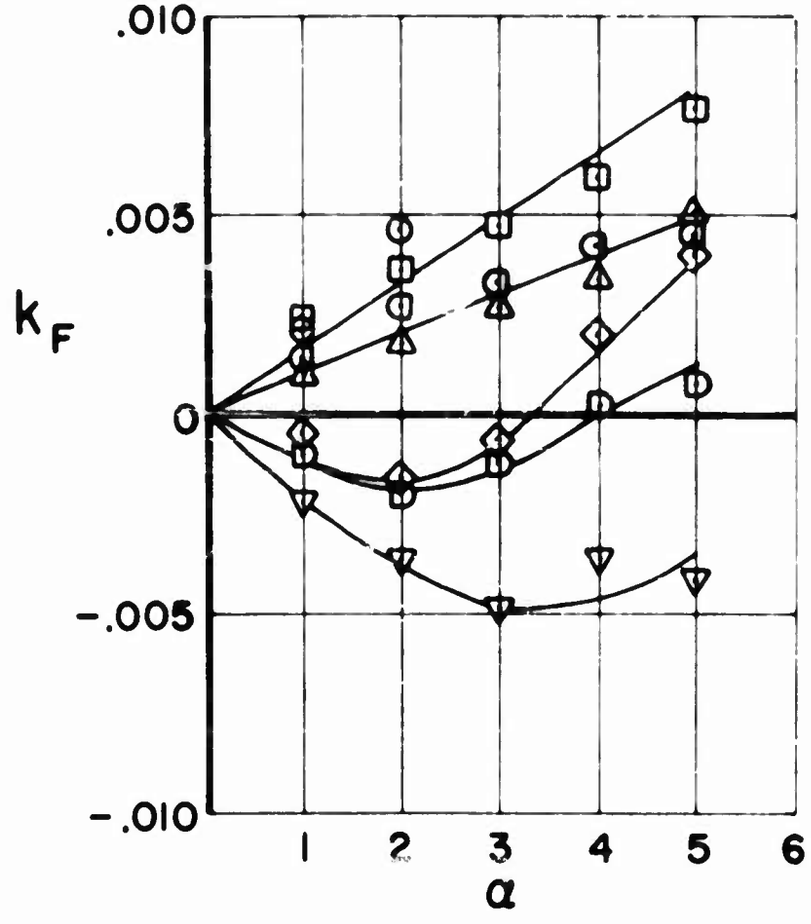

□ BASIC BODY
△ BLUNT NOSE AND ROTATING BAND
○ BLUNT NOSE
◻ CRIMPING GROOVE
◇ ROUNDED BASE
◗ CRIMPING GROOVE & ROUNDED BASE
▽ BLUNT NOSE, ROTATING BAND, CRIMPING GROOVE, & ROUNDED BASE

FIG. 16

THE EFFECT OF A ROUNDED BASE ON MAGNUS FORCE

$M_\infty = 2.0$ $R_\theta = .65 \times 10^6$ $\frac{\omega d}{U} = .30$

FORCED TRANSITION, $\frac{x}{d} = .75$ *40 EMERY

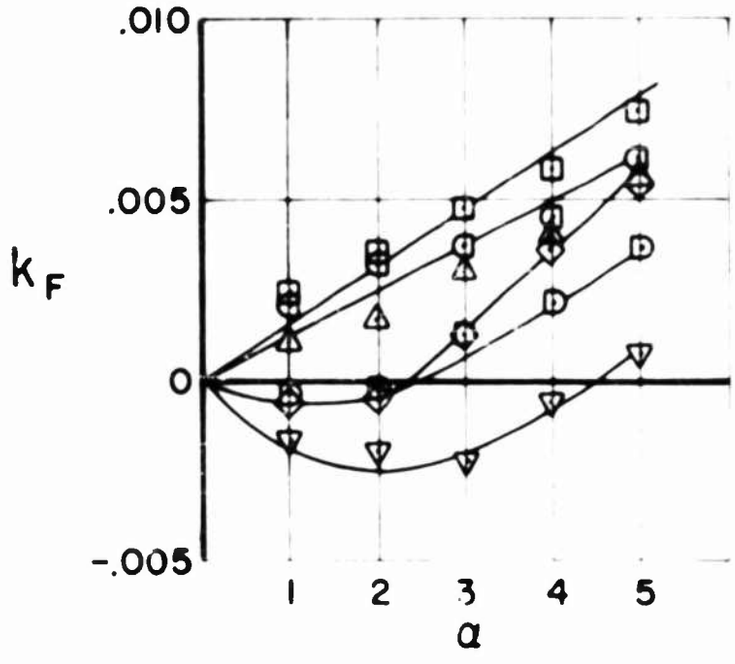

□ BASIC BODY
△ BLUNT NOSE AND ROTATING BAND
○ BLUNT NOSE
◁ CRIMPING GROOVE
◇ ROUNDED BASE
▷ CRIMPING GROOVE & ROUNDED BASE
▽ BLUNT NOSE, ROTATING BAND, CRIMPING GROOVE, & ROUNDED BASE

FIG. 17

THE EFFECT OF A ROUNDED BASE ON MAGNUS FORCE

$M_d = 2.0$ $R_e = .65 \times 10^6$ $\frac{\omega d}{U} = .40$

FORCED TRANSITION AT $\frac{X}{d} = .75$ #40 EMERY

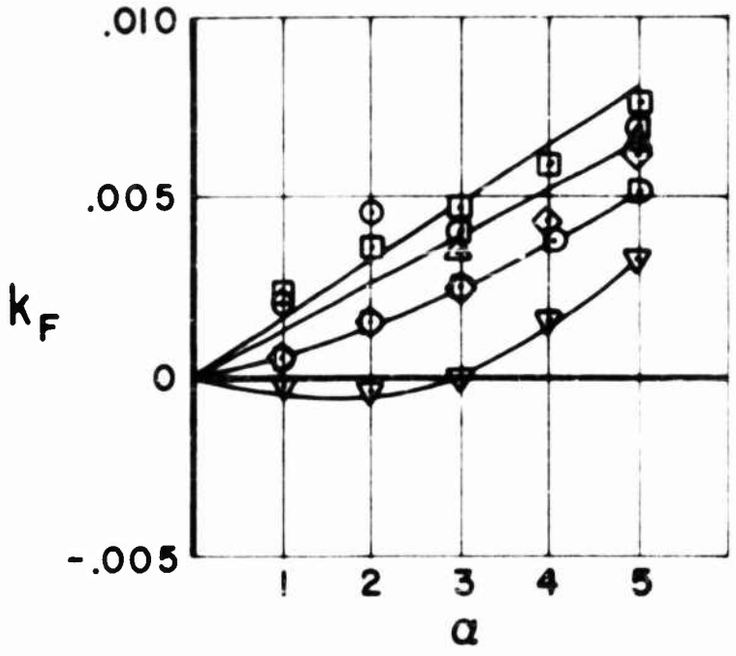

□ BASIC BODY
△ BLUNT NOSE AND ROTATING BAND
○ BLUNT NOSE
◁ CRIMPING GROOVE
◇ ROUNDED BASE
▷ CRIMPING GROOVE & ROUNDED BASE
▽ BLUNT NOSE, ROTATING BAND, CRIMPING GROOVE, & ROUNDED BASE

FIG. 18

THE MAGNUS FORCE ON A ROUNDED BASE MODEL HAVING A LAMINAR BOUNDARY LAYER

$M_d = 2.0$ $R_e = .65 \times 10^6$

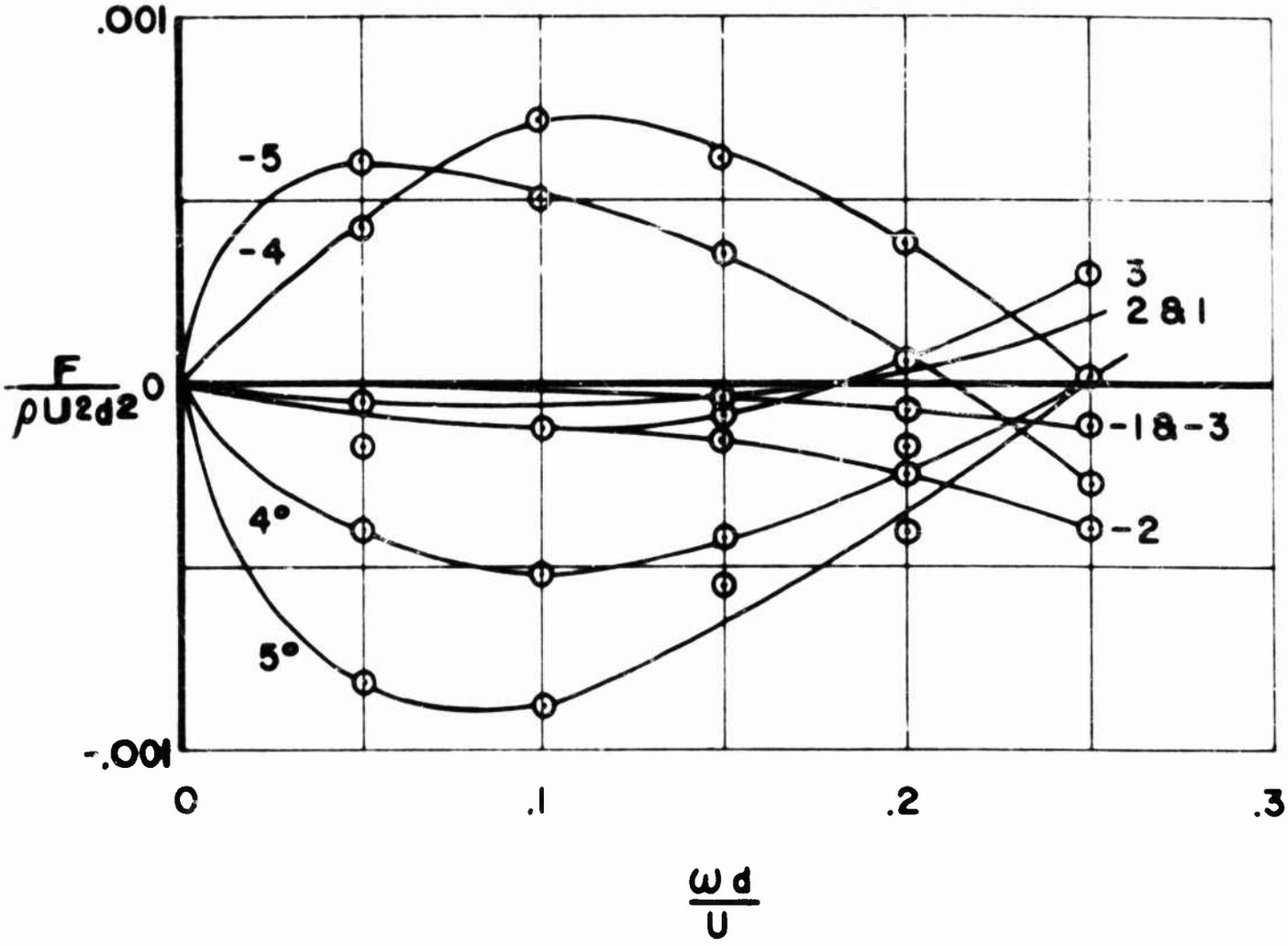

FIG. 19

MAGNUS MOMENT COEFFICIENT
vs.
MACH NUMBER

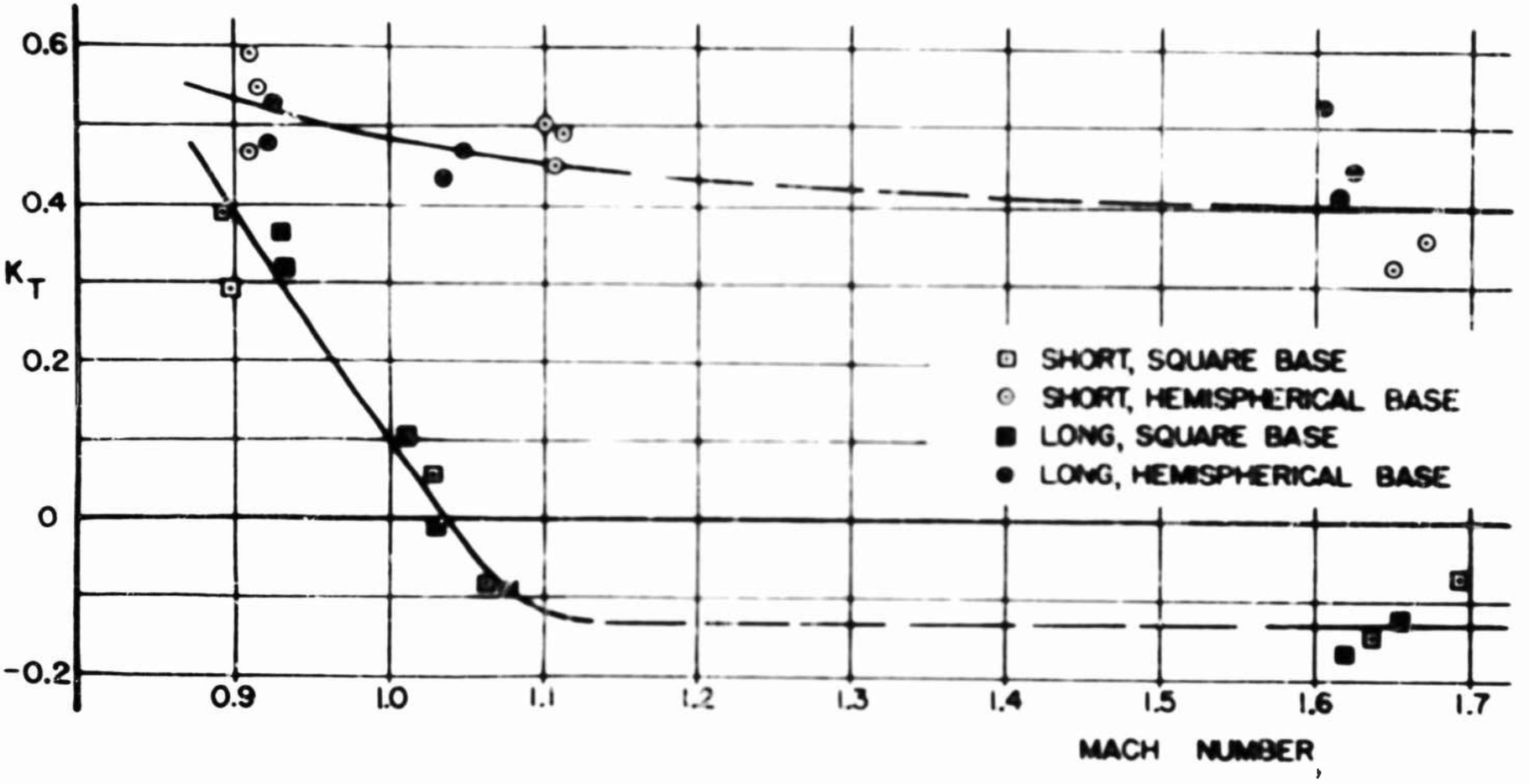

FIGURE 40

Rd. 3454 - LS M = 1.64

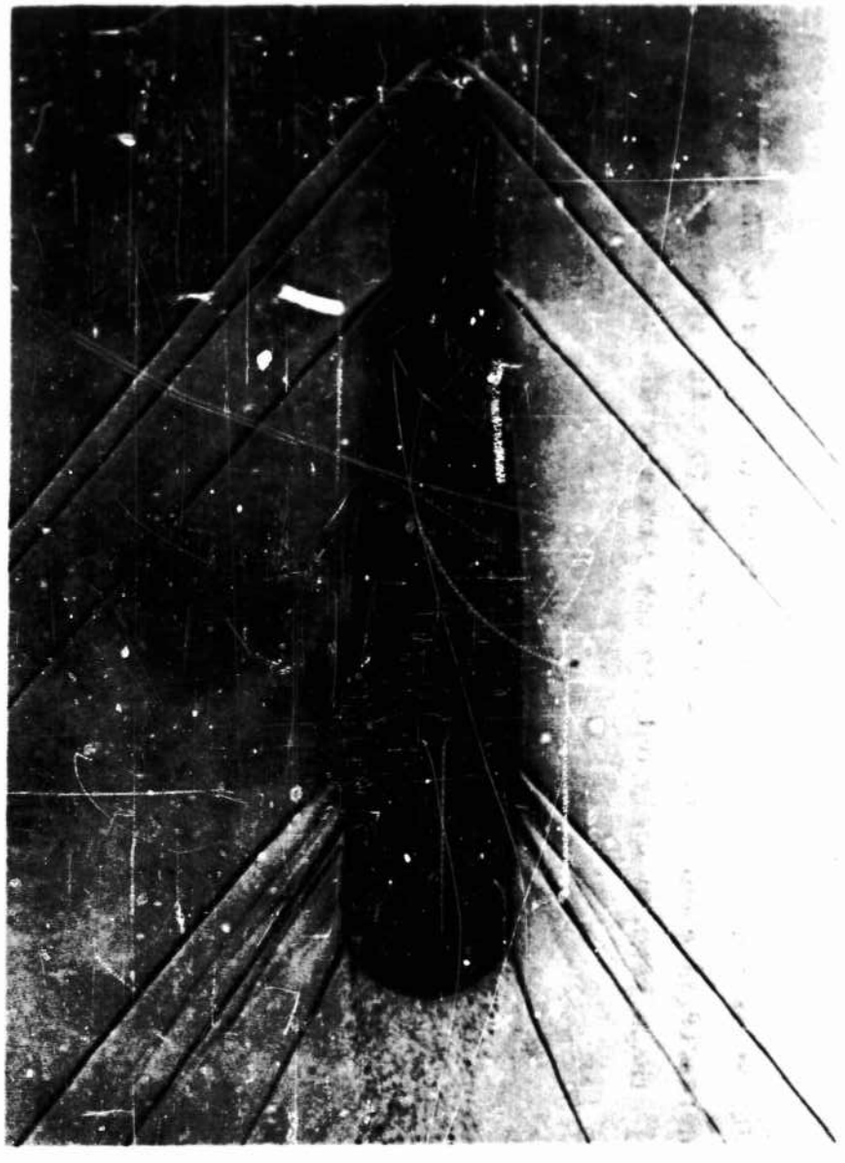

Rd. 3451 - LE M = 1.65

FIGURE 21

APPENDIX I

UNCLASSIFIED RESULTS OF BRL REPORT 994

For those readers who do not have immediate access to BRL Report 994 the unclassified results which are pertinent to this report are listed below. These results apply only to the 30mm aircraft bullet shown in Figure 13.

1. The Magnus force is non-linear with angle of attack (Figure 14).

2. The Magnus force and moment are negative at small angles of attack and most spin rates (Figure 15).

3. The Magnus force and moment are non-linear with spin at low angles of attack ($\alpha \angle 7\text{-}1/2^{\circ}$) (Figure 15).

4. The Magnus force center of pressure is located behind the center of gravity (1.3 cal. forward of the base).

APPENDIX II

SPINNING MODEL INSTRUMENTATION

The air motor is an integral part of the model, the model forming the outside surface of the revolving portion of the motor. This portion of the motor is mounted on the bearing outer races as shown in Figure 22. The inner races of the bearing are mounted on a cylinder which in turn is mounted on the upstream end of the model strain gage balance and supporting strut. The model is rotated by an impulse air turbine with the turbine buckets being mounted in the model base and the air nozzles, of which there are four, being mounted just upstream of the buckets on the supporting strut. An axial hole drilled in the supporting strut serves as a passage for the high pressure air to the nozzles; at the usual test conditions the flow out of the nozzles should be approximately Mach number 4. Since the nozzle air is exhausted into the tunnel, dry air from the wind tunnel storage sphere is used as the high pressure source.

For these tests sufficient power to operate the motor easily was obtained by using a supply pressure of 175 psi. Under the test conditions the motor has a starting torque of 1.2 in. lbs. and develops .5 HP at 45,000 RPM. The acceleration time from 0 to 45,000 RPM is approximately 30 sec.

A spring is used to preload the bearings so that the bearings are subjected to a thrust at all times. The preload appears to confine the ball rotation to one axis, because a track is worn into the ball surface after several thousand revolutions, Figure 23. A thermocouple is mounted near the forward end of the strut so that the temperature rise of the strut can be measured when the model is spun. While breaking in a set of bearings, the appearance of a well worn track is indicated by a leveling off or decrease in the temperature of the forward end of the strut. After several minutes of running at low speeds the temperature stops rising and may in the case of an extremely good bearing start decreasing. Bearings

are broken in by measuring the strut temperature at 10,000 and 20,000 RPM and no bearings are run at higher speeds until no temperature increase is obtained at the low speeds. If the preload is removed from the bearing, the bearing balls will reorient themselves and a rebreaking in of the bearing is necessary.

Measurement of the temperature of the forward end of the strut is also necessary during the tunnel tests for it indicates the condition of the bearings during any one spin period. If the temperature rise becomes excessive or if the temperature of the strut rises above 150°F the bearings are rinsed in a clear solvent and regreased. The 150°F limit was found to be just under the temperature at which freezing of the bearings might occur.

Two permanent magnets are mounted near the base of the model (see Figure 22). As the model rotates, the magnetic field generates a current in a coil mounted on the stationary strut. Using suitable circuitry, the resultant coil signal is converted into a signal proportional to the RPM of the model.

Dynamic balancing of the model is accomplished using a sensitive balancing rig which determines the location and amount of metal to be removed from both the nose and tail of the model. The balancing reduces the wear on the bearings especially at resonant speeds and reduces the strain gage signal oscillations at resonant speeds. Necessarily, readings are not taken near the resonant points.

Temperature compensation of the strain gage bridges was accomplished by varying the resistance of one of the bridge legs until the bridge indicated no unbalance when the temperature of the beam was changed. During test, temperature non-uniformity of the beam caused by heat from the bearings might still cause trouble, so as a check, the bridge unbalance was observed as the model spin varied from 45,000 RPM to 0 under no flow conditions. No bridge unbalance was found, except at resonant speeds, so the method of temperature compensation was considered satisfactory.

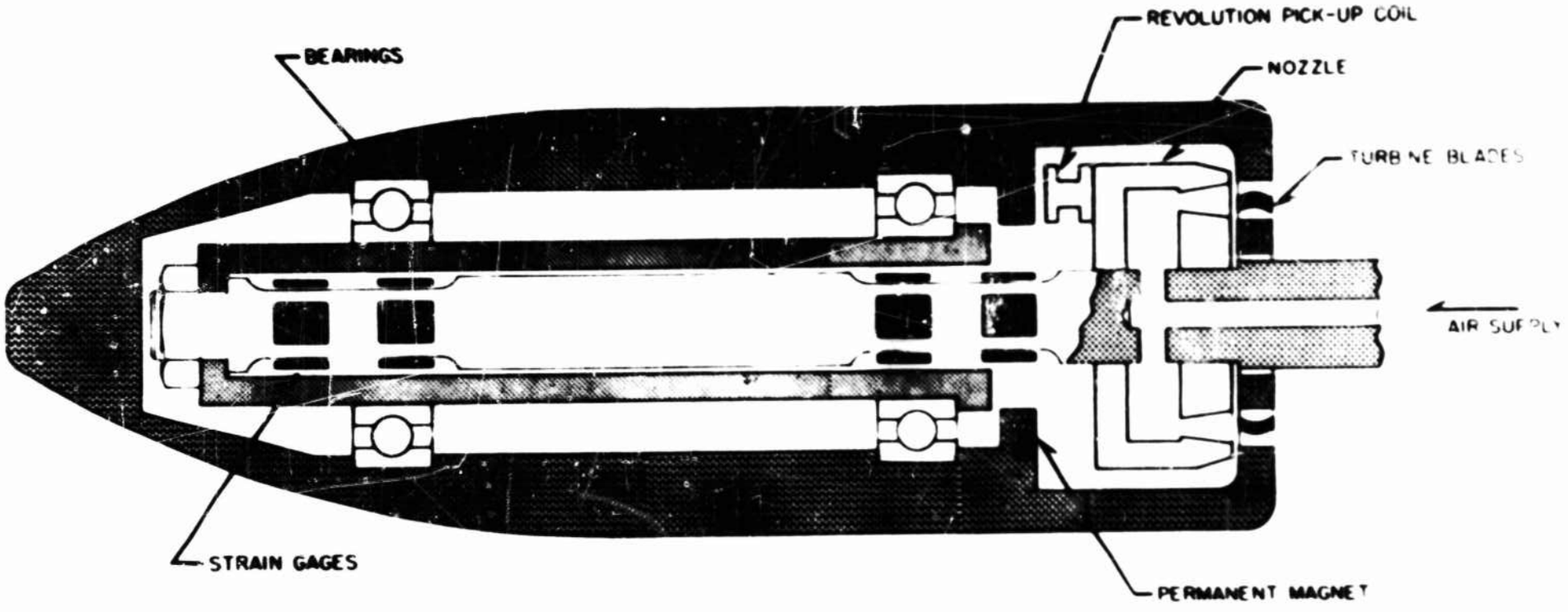

Fig. 22 Spinning Model - Instrumentation

Fig. 23 Ball Bearing After Break in Period

DISTRIBUTION LIST

No. of Copies	Organization
1	Chief of Ordnance Department of the Army Washington 25, D. C. Attn: ORDTB - Bal Sec
1	Commanding Officer Diamond Ordnance Fuze Laboratories Washington 25, D. C. Attn: ORDTL - 012
10	Director Armed Services Technical Information Agency Arlington Hall Station Arlington 12, Virginia Attn: TIPCR
1	Office of Technical Services Department of Commerce Washington 25, D. C.
10	British Joint Services Mission 1800 K Street, N. W. Washington 6, D. C. Attn: Reports Officer
4	Canadian Army Staff 2450 Massachusetts Avenue Washington 8, D. C. Of Interest to: Dr. G. V. Bull CARDE
3	Chief, Bureau of Ordnance Department of the Navy Washington 25, D. C. Attn: ReO
1	Commander U. S. Naval Ordnance Test Station China Lake, California Attn: Dr. H. R. Kelly
2	Commander Naval Ordnance Laboratory White Oak Silver Spring, Maryland Attn: Dr. Kurzweg Dr. E. Krahn
1	Naval Supersonic Laboratory Massachusetts Institute of Technology Cambridge 39, Massachusetts Attn: Mr. Frank H. Durgin
2	Commander Air Proving Ground Center Eglin Air Force Base, Florida Attn: Dr. Alan Galbraith Mr. Foster Burgess
3	Director National Aeronautics and Space Agency Langley Field, Virginia Attn: Mr. J. Bird Mr. C. E. Brown Dr. A. Buseman
1	Director National Aeronautics and Space Agency Lewis Flight Propulsion Laboratory Cleveland Airport Cleveland, Ohio Attn: Dr. Evaard
3	Director National Aeronautics and Space Agency Ames Laboratory Moffett Field, California Attn: Dr. A. C. Charters Mr. H. J. Allen Dr. A. Eggers

DISTRIBUTION LIST

No. of Copies	Organization
1	Director National Bureau of Standards Connecticut Ave. & Van Ness St., N. W. Washington 25, D. C. Attn: Mr. G. B. Schubauer
10	Office of Ordnance Research Box C. M. Duke Station Durham, North Carolina
1	Jet Propulsion Laboratory 4800 Oak Grove Drive Pasadena 2, California Attn: Dr. F. Goddard
1	Aero Physics Development Corp. P. O. Box 657 Pacific Palisades, California Attn: Dr. William Bollay
1	The Eglin Corporation 2925 Merrill Road P. O. Box 13214 Dallas 20, Texas Attn: Dr. Floyd L. Cash
1	Cornell University Graduate School of Aeronautical Engineering Ithaca, New York Attn: Dr. W. R. Sears
2	Princeton University Aeronautics Department Forrestal Research Center Princeton, New Jersey Attn: Prof. S. Bogdonoff Prof. W. Hayes
1	University of Texas Defense Research Laboratory 500 East 24th Street Austin, Texas Attn: Mr. J. B. Oliphint

No. of Copies	Organization
1	Guggenheim Aeronautical Laboratory California Institute of Technology Pasadena 4, California Attn: Prof. H. W. Liepman
1	Dr. R. Bolz Case Institute of Technology Cleveland, Ohio
1	Professor Francis H. Clauser, Jr. Chairman, Department of Aeronautics Johns Hopkins University Baltimore 18, Maryland
1	Professor G. Carrier Division of Applied Sciences Harvard University Cambridge 38, Mass.
1	Professor H. W. Emmons Harvard University Cambridge 38, Mass.
1	Professor C. B. Millikan Guggenheim Aeronautical Laboratory California Institute of Technology Pasadena 4, California
1	Office Chief of Staff, USA Res. & Dev. Washington 25, D. C. Attn: Army Research Office
98	GM/MML - 200/16 LIST NO. 16 PART A

DISTRIBUTION LIST

No. of Copies	Organization
	ABSTRACT CARDS ONLY for the following
1	Allegany Ballistic Laboratory Cumberland, Maryland
2	Budd Company Red Lion Plant Philadelphia 15, Pa Attn: Mr. C. B. Willman, Weapons Div. Mr. A. F. Stranges, Weapons Div.
1	Capehart-Farnsworth Corp. Fort Wayne, Indiana Attn: Mrs. Margaret Moyer
1	Chamberlain Corporation Waterloo, Iowa Attn: Mr. Irving Herman
1	ARO, Inc. P. O. Box 162 Tullahoma, Tennessee Attn: Mr. R. Smelt
1	Douglas Aircraft Company Santa Monica, California Attn: Mr. W. S. Cohen
1	General Electric Company Research Laboratory Schenectady, New York Attn: Library
1	Grumman Aircraft Engineering Corp. Bethpage, New York Attn: Mr. C. Tilgner, Jr.
1	North American Aviation, Inc. Aeronautical Laboratory Downey, California Attn: Dr. E. C. Van Driest
1	Ramo-Wooldridge Corporation 409 East Manchester Blvd. Inglewood, California Attn: Dr. Louis G. Dunn
1	The Rand Corporation 1700 Main Street Santa Monica, California Attn: Librarian
1	United Aircraft Corporation East Hartford, Connecticut Attn: Mr. M. Schweiger
1	Brown University Graduate Div. of Applied Mathematics Providence 12, Rhode Island Attn: Dr. R. Probstein
1	University of California at Berkeley Berkeley, California Attn: Prof. S. A. Schaaf
1	University of California at Los Angeles Department of Engineering Los Angeles 24, California Attn: Dr. L. M. Boelter
1	Case Institute of Technology Cleveland, Ohio Attn: Dr. G. Kuerti
1	Catholic University of America Department of Physics Washington 17, D. C. Attn: Prof. K. F. Herzfeld Prof. M. Monk
1	Cornell Aeronautical Laboratory Buffalo, New York Attn: Dr. A. Flaz Dr. Ira G. Ross

DISTRIBUTION LIST

No. of Copies	Organization
1	Cornell University Graduate School of Aeronautical Engineering Ithaca, New York Attn: Dr. A. Kantrowitz
1	Harvard University Dept. of Applied Physics & Engineering Science Cambridge 38, Mass. Attn: Dr. A. Bryson
1	The Johns Hopkins University Dept. of Mechanical Engineering Baltimore 18, Maryland Attn: Dr. S. Corrsin
1	The Johns Hopkins University Department of Aeronautical Engr. Baltimore 18, Maryland Attn: Dr. L. Kovasznay
1	Lehigh University Physics Department Bethlehem, Pennsylvania Attn: Dr. R. Emrich
1	University of Maryland Institute of Fluid Dynamics & Applied Mathematics College Park, Maryland Attn: Director
1	University of Maryland Dept. of Aeronautical Engrg. College Park, Maryland Attn: Dr. S. F. Shen
1	Massachusetts Institute of Technology Department of Aeronautical Engineering Cambridge 39, Massachusetts Attn: Prof. J. R. Markham
1	University of Michigan Dept. of Aeronautical Engrg. East Engineering Building Ann Arbor, Michigan Attn: Dr. Arnold Kuethe
1	University of Minnesota Dept. of Aeronautical Engrg. Minneapolis 14, Minnesota Attn: Dr. R. Hermann
1	University of Minnesota Dept. of Mechanical Engrg. Division of Thermodynamics Minneapolis, Minnesota Attn: Dr. E. R. G. Eckert
1	National Science Foundation Washington 25, D. C. Attn: Dr. R. Seeger
1	New York University Department of Aeronautics University Heights New York 53, New York Attn: Dr. J. F. Ludloff
1	New York University Institute of Mathematics & Mechanics 45 Fourth Street New York 53, New York Attn: Dr. R. W. Courant
1	North Carolina State College Dept. of Engineering Raleigh, North Carolina Attn: Prof. R. M. Pinkerton
1	Ohio State University Aeronautical Engineering Dept. Columbus, Ohio Attn: Prof. G. L. von Eschen

DISTRIBUTION LIST

No. of Copies	Organization
1	Pennsylvania State College Dept. of Aeronautical Engrg. State College, Pennsylvania Attn: Prof. M. Lessen
1	Polytechnic Institute of Brooklyn Aerodynamic Laboratory 527 Atlantic Avenue Freeport, New York Attn: Dr. A. Ferri
1	Princeton University Forrestal Research Center Princeton, New Jersey Attn: Library
1	Rensselaer Polytechnic In... Aeronautics Department Troy, New York Attn: Dr. R. T. Harrington
1	University ... ington Dept. of Aeronautical Engrg. ...tle 5, Washington Attn: Prof. R. E. Street
	...versity of Illinois Dept. of Aeronautical Engrg. Urbana, Illinois Attn: Prof. C. H. Fletcher
1	Institute of the Aeronautical Sciences 2 East 64th Street New York 21, New York Attn: Library
1	Midwest Research Institute 4049 Pennsylvania Kansas City 11, Missouri Attn: Mr. M. Goland, Director for Engr. Sciences
1	Professor J. W. Beams Rouse Physical Laboratory University of Virginia Charlottesville, Virginia
1	Professor J. O. Hirschfelder University of Wisconsin Department of Chemistry Madison, Wisc...
1	Professor William Prager Chairman, Physical Sciences Council Brown University Providence 12, Rhode Island
68	GM/MML - 200/16 LIST NO. 16 PART C & DA

ARMY-APG, Md.-D

NOTIFICATION OF MISSING PAGES

INSTRUCTIONS: THIS FORM IS INSERTED INTO ASTIA CATALOGED DOCUMENTS TO DENOTE MISSING PAGES.

AD No. 212064
ASTIA FILE COPY

CLASSIFICATION (CHECK ONE)		
UNCLASSIFIED	CONFIDENTIAL	SECRET
✓		

THE PAGES, FIGURES, CHARTS, PHOTOGRAPHS, ETC., MISSING FROM THIS DOCUMENT ARE:

MISSING PAGES ARE BLANK

DO NOT REMOVE